

ITC 1/53 Information Technology and Control Vol. 53 / No. 1 / 2024 pp.302-316 DOI 10.5755/j01.itc.53.1.34536	Dual Attention Aware Octave Convolution Network for Early-Stage Alzheimer's Disease Detection	
	Received 2023/07/03	Accepted after revision 2024/01/10
	HOW TO CITE: Rangaraju, B., Chinnadurai, T., Natarajan, S., Raja, P. V. (2024). Dual Attention Aware Octave Convolution Network for Early-Stage Alzheimer's Disease Detection. <i>Information Technology and Control</i> , 53(1), 302-316. https://doi.org/10.5755/j01.itc.53.1.34536	

Dual Attention Aware Octave Convolution Network for Early-Stage Alzheimer's Disease Detection

Banupriya Rangaraju

Department of Computer Science and Engineering, K. S. R College of Engineering, Tiruchengode, 637215, India

Thilagavathi Chinnadurai

Department of Information Technology, M.Kumarasamy College of Engineering, Karur, 639113, India

Sarmiladevi Natarajan

Department of Artificial Intelligence and Data Science, Kongunadu College of Engineering and Technology, Trichy, 621215, India

Vishnu Raja

Department of Computer Science and Engineering, Kongu Engineering College, Erode, 638060, India

Corresponding author: rbanupriyares1@outlook.com

Some of the most fundamental human capabilities, including thought, speech, and movement, may be lost due to brain illnesses. The most prevalent form of dementia, Alzheimer's disease (AD), is caused by a steady decline in brain function and is now incurable. Despite the challenges associated with making a conclusive diagnosis of AD, the field has generally shifted toward making diagnoses justified by patient records and neurological analysis, such as MRI. Reports of studies utilizing machine learning for AD identification have increased in recent years. In this publication, we report the results of our most recent research. It details a deep learning-based, 3D brain MRI-based method for automated AD detection. As a result, deep learning models have become increasingly popular in recent years for analyzing medical images. To aid in detecting Alzheimer's disease at an initial phase, we suggest a novel dual attention-aware Octave convolution-based deep learning network (DACN). The three main parts of DACN are as follows: First, we use Patch Convolutional Neural Network (PCNN) to identify discriminative features within each MRI patch while simultaneously boosting the features of abnormally al-

tered micro-structures in the brain; second, we use an Octave convolution to minimize the spatial redundancy and widen the field of perception of the brain's structure; and third, we use a dual attention aware convolution classifier to dissect the resulting depiction further. An outstanding test accuracy of 99.87% is reached for categorizing dementia phases by employing the suggested method in experiments on a publicly available ADNI (Alzheimer's Disease Neuroimaging Initiative) dataset. The proposed model was more effective, efficient, and reliable than the state-of-the-art models through our comparisons.

KEYWORDS: Alzheimer's disease, Brain disorder, deep learning, depth-wise separable convolution, spatial attention blocks.

1. Introduction

Human capabilities such as thought, speech, and movement are fundamental to our daily lives. However, brain illnesses can rob individuals of these abilities, profoundly influencing their standard of living. One of the most prevalent and devastating forms of brain disease is AD, marked by a gradual loss of mental capacity. Unfortunately, AD has no cure, making early detection crucial for managing the condition effectively. As the human population ages, neurological disorders like Alzheimer's and Parkinson's become more common. Alzheimer's disease (AD) stands out among these disorders due to its high prevalence: 5.5% in Europe in 2016 [27] and 10% in the USA in 2019 [10]. The primary difficulty Alzheimer's disease researchers confront today is making a definitive premortem diagnosis. There is still a lot we do not know about this condition beyond the fact that it causes shifts in the brain's cortex and is associated with mood swings that are not related to normal aging [35, 9]. Though the exact reasons for AD remain unclear, most scientists think it is due to hereditary and environmental factors. Some research has linked it to periodontal disease-causing bacteria [6] and herpes simplex virus type 1 [17]. There may be sexual dimorphism in the occurrence of the illness [8], and it is thought to be age-related but not age-dependent [4]. Because of its lasting effects on society and researchers' inability to agree on its cause, the illness is still a topic of intensive investigation.

Alzheimer's disease affects the brains with larger ventricles and smaller cerebral cortex and memory. When the brain's hippocampus is shrunk, it causes spatial and episodic memory problems. It's a link between your head and your body. Loss of hippocampal volume is associated with the deterioration of synapses and neuronal terminals [38]. Uncertainty between neurons has been linked to problems in

short-term memory, organizing, and reasoning [34]. Experts in the field have created many computerized diagnostic systems (CADS) for reliable identification and categorization of AD-related extracted characteristics [15]. Otherwise, more work and time on the part of human specialists is needed to process the retrieved information. To remove the features directly from medical pictures, researchers have recently developed deep-learning models/techniques [22]. The field of medical imaging, including CT, MRI, X-ray, microscope, and mammography, has been primarily conquered by deep learning models [14]. Most of these models and techniques relied on binary categorization, which reveals whether the patient has AD [19]. However, the phases of dementia must be identified for an accurate diagnosis. Ten to sixteen percent of people with MCI rapidly progress to AD per year [16], making it a severely impaired stage compared to AD. Stabilization or reversal to the healthy stage in MCI patients is extremely varied [33]. The multi-modal information about the brain's function and organization contained in MRI scans makes them ideal for medical care.

Traditionally, diagnosing AD has been challenging, relying on medical past and neuropsychological evidence with MRI. Yet, there has been an increasing amount of study lately exploring the application of machine learning techniques to aid in AD identification.

Motivation: Alzheimer's Disease is a progressive and debilitating neurological condition, and early detection is crucial for timely intervention and treatment. Detecting AD at its initial stages can significantly improve the quality of life for affected individuals and potentially slow down the progression of the disease. Research in this area aims to develop more accurate and efficient methods for early diagnosis. Advance-

ments in medical imaging technology have provided researchers with a wealth of brain image data. Leveraging these technologies and analyzing the images with the help of artificial intelligence and deep learning models can lead to more accurate and consistent diagnostic tools for AD. Traditional methods of diagnosing AD often involve subjective assessments by healthcare professionals. These assessments may vary from one clinician to another and can be influenced by individual experience and biases. The motivation behind this research is to develop objective and data-driven approaches that can provide consistent and reliable diagnostic results.

This paper offers the results of our latest research, which introduces a novel deep learning-based method for the automated detection of AD using 3D brain MRI data. Deep learning models have gained significant popularity in medical image analysis due to their ability to extract intricate patterns and features from complex data. To enhance the early detection of Alzheimer's disease, we propose a novel deep learning network called the Dual Attention Aware Depth Wise Separable Convolution (DA-DSC) network. The main contribution of our is as follows.

- 1 we employ PCNN equipped to identify discriminative features within each MRI patch. This approach allows us to simultaneously emphasize the features of abnormally altered micro-structures in the brain, potentially indicative of AD progression.
- 2 we use an Octave convolution to minimize spatial redundancy and widen the field of perception of the brain's structure.
- 3 we leverage a dual attention-aware convolution classifier to analyze the resulting representation further and make a robust diagnosis. By utilizing this architecture, we aim to achieve improved accuracy, efficiency, and reliability compared to existing state-of-the-art models.

To evaluate the efficiency of our proposed technique, we conducted experiments on a publicly available dataset. Remarkably, our suggested model achieved outstanding test accuracy in categorizing dementia phases. These impressive consequences establish the potential of our method for accurate and early detection of Alzheimer's disease. Compared with existing models, our proposed DA-DSC network proves to be more effective, efficient, and reliable. The results of

this investigation add to the burgeoning literature on machine learning techniques in the field of AD diagnosis and pave the way for improved patient care and management of this debilitating disease.

The same structure applies to the remaining parts of this article. Section 3 discusses relevant literature and presents the proposed model. Section 4 details the findings of the inquiry. The conclusion and next steps are outlined in Section 5.

2. Related Works

Research has proposed several methods of identifying AD and prognosis based on categorization. Below is a summary of current revisions that have used conventional ML and DL methods in AD detection technologies. Earlier research on Alzheimer's disease diagnosis has used more traditional machine-learning approaches. There is model building to interpret MRIs and other pictures of the brain's anatomy and structure and the brain's activity to diagnose disease. Furthermore, it relied mainly on manually constructed features and visualizations of features compared to voxel, region, or patch-based approaches and treated segmentation challenges as classification concerns. It took more time and many expertly segmented pictures to train classification algorithms.

Many applications of artificial intelligence models have been suggested to extract characteristics and transfer out frequent procedures on AD MRI images. To detect individuals with AD from T1-weighted MRI images, Kloppel et al. [21] developed a dimensional compression model based on a linear support vector machine technique. A multimodal classification for AD was developed by Gray et al. [11] using PET and MRI data using a random forest classifier. Morra et al. [25] compared models for detecting AD in MRI images, including support vector machine and hierarchical AdaBoost models. Using shrunken kernel principal component analysis (DKPCA) and SVM, Neff et al. [26] devised an approach for feature extraction and reduction in AD MRI images. Using a multi-support vector machine (MSVM) kernel, they evaluated the model on the OASIS datasets and found it to be 92.5% accurate. Wang et al. [40] extracted and categorized the structures in MRI data using wavelet entropy and biography-based optimizers.

They achieved perfect accuracy by using a 6-fold CV model to 64 brain pictures. Ben Ahmed et al. [3] have enhanced the precision of feature extraction and feature selection on datasets of Alzheimer's disease and neurodegenerative disease patients. They turned to SVM, the gray level occurrence matrix, and voxel-based morphometric (VBM) analysis for feature extraction and classification. Over 92% accuracy was achieved when tested on data from the ADNI. The Harvard Medical School has created systems for extracting and reducing features from T2-weighted MRI scans, as proposed by El-Dashan et al. [7]. Hinrich et al. [13] used the suggested method to multi-classify Alzheimer's disease using data from the ADNI database. All in all, a total of 79.8 percent accuracy was achieved. The correlation between subjects was also discovered by Yue et al. [39] using a voxel-based hierarchical feature extraction method. Second, we processed the feature using feature vectors and sent them into a classifier to see how well it performed. To diagnose the various phases of AD, Ahmed et al. [1] created a more straightforward CNN model based on the patch-based classifier. The model both improved accuracy and decreased computing time.

A model for the early detection, categorization, forecasting, and identification of AD, MCI, and aged cognitively normal from those with MCI was proposed by Rallabandi et al. [31]. Including 371 healthy controls, 328 patients with moderate dementia, 169 with severe dementia, and 284 with dementia, the ADNI database provided 1167 participants with whole-brain MRIs. Using FreeSurfer evaluation, they were able to identify 68 features related to the thickness of the cortical from each image. When handling sequential data, recurrent neural networks, particularly those with long short-term memory (LSTM), are powerful models [36]. The vanishing gradient problem is fixed, feature propagation is strengthened, and the number of parameters is decreased thanks to the DenseNet CNN architecture. Therefore, it was adopted to extract the interslice features [37].

Considering all of this information, we present a new Deep Learning (DL) model that layers an LSTM on top of the bottleneck features retrieved using the initialized weights of a previously trained CNN based on the DenseNet architecture and fed with data from ImageNet. CNN and LSTM are used in this hybrid model

to learn both interslice and interslice characteristics from brain MRI scans. For the diagnosis of Alzheimer's disease in its earliest stages, the author [2] suggests a hybrid Deep Learning Approach. Combining MRI, PET, and traditional neuropsychological test scores is one approach to early AD identification utilizing multimodal imaging and CNN with the LSTM algorithm. Better prediction performance in Alzheimer's disease diagnosis is sought in this study [32] by proposing an integrated multi-solutional ensemble deep learning-based approach.

Martinez-Murcia et al. [24] employ deeper convolutional autoencoders to study AD data processing. Extracting MRI features that stand in for cognitive indications and the underlying neurodegenerative process is now possible because of the data-driven deconstruction of MRI scans. A DNN with interconnected layers [30, 12] accomplishes binary arrangement. There is a unique activation function for each of the underlying hidden layers. After doing k-folds validation, a model with the maximum presentation is selected. The Lancet Commission reported that it is possible to alter 35 percent of the risk factors for developing Alzheimer's disease. A high correlation is shown among genetic examinations. Biomarker and neuropsychological results when data from the ADNI trial is used using ten-fold cross-validation [20].

3. Methods and Materials

AD is diagnosed using brain MRI by experienced physicians. Neurological disorders are challenging to predict in the early stages. The training and optimization process for the neural network and the technology behind related approaches such as CNN and Patch-Nets are presented here.

Next, the data must be labeled appropriately, a crucial step in supervised learning. Expert clinicians or neurologists review the MRI scans and assign labels indicating whether the individual has Alzheimer's Disease or is part of the healthy control group. This labeling process ensures the availability of ground truth information for training the deep learning model. When detecting dementia in its earliest stages, the deep learning model is crucial. It leverages advanced algorithms, such as the suggested dual at-

attention-aware convolution-based deep learning network, to learn compound patterns and structures from the pre-processed and labeled MRI data. The model is trained using a combination of MRI patches, spatial attention blocks, and attention-aware convolution, which collectively enable the identification of discriminative features and abnormal microstructures associated with AD.

Classification is a vital step in the process, where the trained deep learning model predicts whether a given MRI scan belongs to a healthy individual or someone with Alzheimer's. The model utilizes the learned representations and weights to make accurate predictions based on the extracted features from the brain structures. Lastly, the recital of the deep learning model needs to be evaluated to assess its effectiveness in early diagnosis. By comparing the model's predictions with the ground truth labels, the performance evaluation provides insights into the accuracy and reliability of the deep learning model for detecting Alzheimer's Disease at an early stage.

3.1. Data Collection

The ADNI dataset is a comprehensive collection of clinical, imaging, genetic, and biomarker data from individuals with Alzheimer's disease, mild cognitive impairment (MCI), and healthy controls. The initiative aims to facilitate research and advancements in understanding, diagnosing, and treating Alzheimer's disease. The site provides access to Alzheimer's disease individuals, moderately impaired individuals, and older controls who participated in the North American ADNI research.

EMCI (Early Mild Cognitive Impairment) stage refers to individuals who are in the cognition decline's first symptoms but do not meet the criteria for a diagnosis of Alzheimer's disease. LMCI (Late Mild Cognitive Impairment) stage represents individuals in a more advanced stage of cognitive decline but still do not meet the standards for analysis of Alzheimer's disease. MCI (Mild Cognitive Impairment) stage encompasses individuals with mild mental damage, an intermediate phase among normal aging and Alzheimer's disease. MCI personalities may have noticeable cognitive decline but still retain functional independence. AD (Alzheimer's Disease) stage represents individuals diagnosed with AD with significant cognitive impairment and functional decline. CN (Cognitively Normal) stage includes individuals with no significant cognitive impairment and is the control group.

As shown in Figure 1, the photos in the dataset range in size. Variations in picture size might lead to inaccuracy in the design. This is why we pre-processed the data. Our data pre-processing consists of two stages: a) image scaling and b) image denoising. Training a neural network model takes less time when images are resized. We used OpenCV Python to resize the photos. Denoising images is a key challenge in artificial intelligence and the processing of pictures. Denoising is a process that estimates the original picture by removing unwanted noise. We ran denoising algorithms on MRI images of the brain from our ADNI dataset to boost our model's accuracy. Python OpenCV3 was used for the denoising process.

Figure 1

Sample images from the dataset ADNI

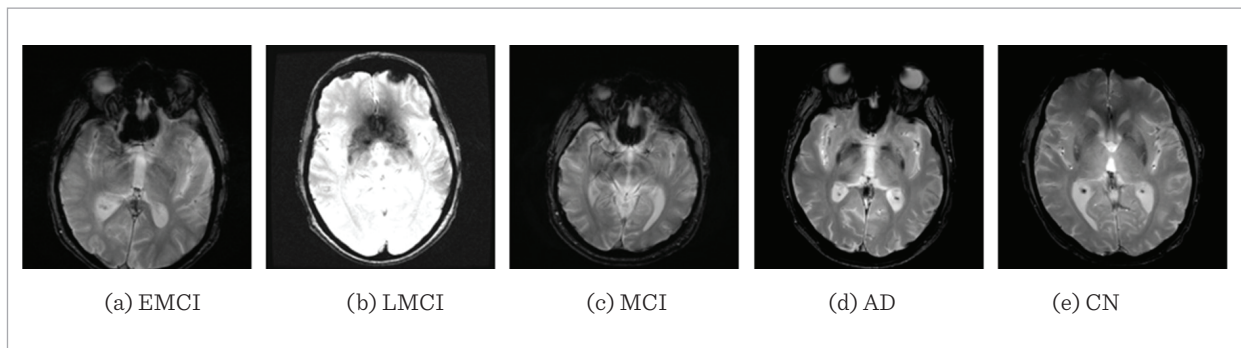
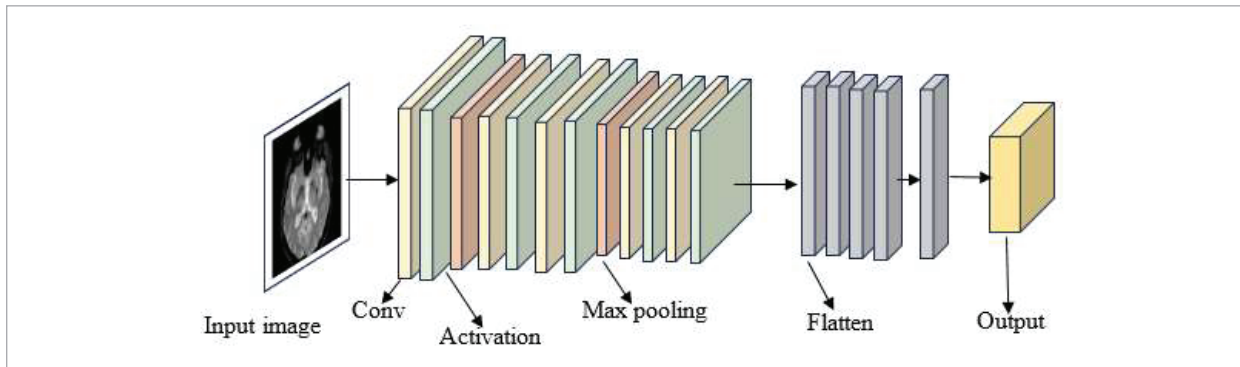


Figure 2

The structure of PCNN architecture



3.2. Methodology

3.2.1. Segmentation by PCNN

A patchwise CNN (PCNN) is a common approach for analyzing brain images in medical imaging. In this approach, the input brain image is divided into smaller patches, and each patch is processed individually by the CNN. The CNN learns patterns and features from these patches to make predictions or perform tasks such as segmentation, classification, or anomaly detection, as shown in Figure 2.

The equation for a PCNN can be represented as follows:

$$Y = f(W * X + b) \quad (1)$$

Where: Y represents the output or prediction made by the CNN, X denotes the input patch, which is a subset of the brain image, W represents the learnable weights of the CNN's convolutional layers. b represents the biases associated with the convolutional layers. $f()$ is the activation function that introduces non-linearity into the system. Convolutional layers then pooling layers make up the PCNN, which extracts hierarchical features from source patches. The data is then put into fully linked layers, flattened and used to produce projections or carry out the desired activities. The final layer of the network often uses a suitable activation function, such as softmax for organization tasks or sigmoid for binary classification. During training, the CNN learns the optimal value for the weights (W) and biases (b) by minimizing a loss function, typically through backpropagation and gradient descent optimization.

3.2.2. Octave Convolution

In particular, 3D CNNs used for image classification have memory requirements and hardware demands that expand dramatically as the number of convolution layers increases. Recently proposed octave convolution [5, 18] divides the CNN-generated feature map into two spatially frequent stages, which are then separately reviewed, swapped, and merged to reduce spatial duplication and expand the observer's field of view.

By learning patterns and features from the data, the system can assess new neuroimaging scans and predict the likelihood of Alzheimer's disease [28-29].

Octave Convolution is a type of convolutional operation that aims to capture both high-frequency and low-frequency information in an image efficiently. It was introduced to address the challenges of capturing multi-scale features in computer visualization responsibilities such as brain image classification. The Octave Convolution operation involves splitting the input image into two paths, as shown in Figure 3: the high-frequency and low-frequency paths. The high-frequency path captures fine-grained details, while the low-frequency path captures the global context and larger-scale features.

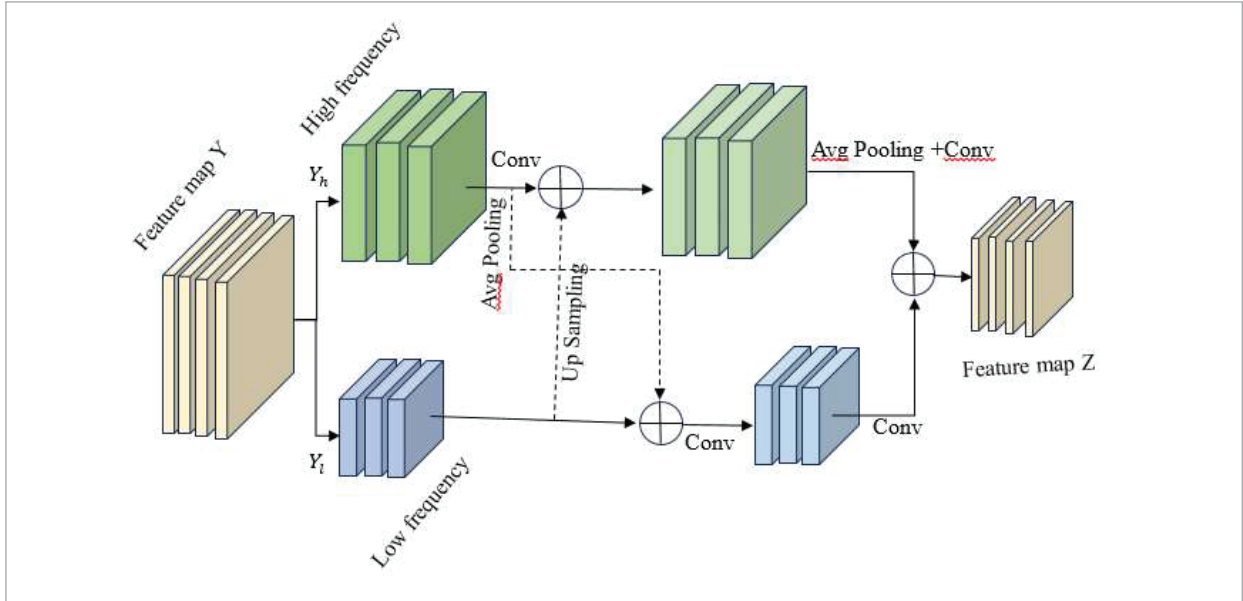
Mathematically, the Octave Convolution can be expressed as follows:

$$Y_h = \sum_{i=0}^n W_h^i * X_h + \sum_{i=0}^m W_h^i * D_h \quad (2)$$

$$Y_l = \sum_{i=0}^n W_l^i * X_l + U * D_h \quad (3)$$

Figure 3

The Octave Convolution architecture



$$Y = \begin{bmatrix} Y_h \\ Y_l \end{bmatrix}, \quad (3)$$

where: Y_h and Y_l are the production feature maps for the high-frequency and low-frequency paths, respectively. Y_h and Y_l are the input feature maps for the high-frequency and low-frequency paths, respectively. W_h^i and W_l^i are the convolutional filters for the high-frequency and low-frequency paths, correspondingly. D_h is the downsampled version of X_h obtained by reducing its spatial resolution. U is an upsampling operation that increases the spatial resolution of D_h to match the size of Y_l . n and m represent the number of high-frequency and low-frequency filters, respectively.

In the Octave Convolution operation, the high-frequency path operates at the original spatial resolution, while the low-frequency path operates at a reduced spatial resolution. The down sampled feature map D_h captures the low-frequency information, which is then up sampled using the Upsampling operation U to match the size of the low-frequency feature map Y_l . The outputs of both paths are concatenated to obtain the final output feature map Y . By splitting the convolution into different frequency paths, Octave Convolution enables the network to effectively cap-

ture multi-scale information, making it suitable for tasks such as brain image classification, where both fine-grained details and global context are essential for accurate classification.

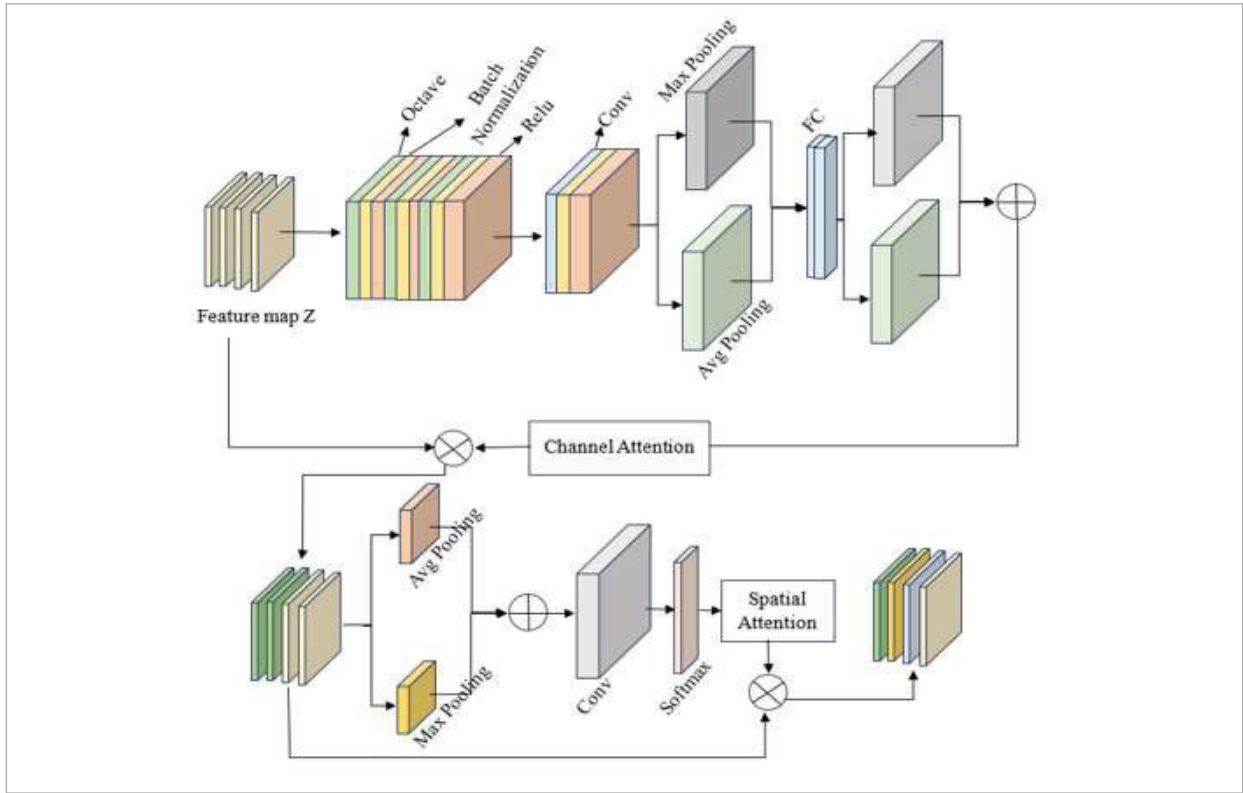
3.2.3. Dual Attention-based Convolution Network (DACN)

The patch output from PCNN is fed into network branches of 3D octave convolution layers to extract multi-scale characteristics. Batch normalization-RELU(BN-RELU) follows the octave 3D convolution layer in the network's fork. It's important to note that the octave 3D convolution kernel widths varied amongst the three branches, each with its unique value. Figure 4 shows several convolution kernels used in constructing each octave of a 3D convolution layer that runs throughout the various branches. To improve the discriminatory power of the resulting feature maps, we use an attention module that combines channel-wise attention with spatial-wise attention. Two FC layers and a softmax classifier are employed as the last step in classification.

Channel Attention and Spatial Attention are two mechanisms commonly used in computer vision tasks, with brain image classification, to improve the representation power of CNNs and focus on relevant

Figure 4

Dual attention-based convolution network (DACN)



features within an image. Channel Attention aims to emphasize or suppress specific channels (or feature maps) in a CNN based on their importance for the given task. It enables the network to attend to informative features while suppressing less relevant ones selectively. Given an input feature map, a global pooling operation (e.g., global average pooling) is applied to aggregate information across spatial dimensions, resulting in a channel descriptor.

The channel descriptor is then passed through one or more fully connected (or convolutional) layers to capture channel-wise relationships and generate attention weights. The attention weights are usually obtained by applying an activation function, such as sigmoid or softmax, to ensure that they represent importance values between 0 and 1. Finally, the attention weights are multiplied element-wise with the original feature map to modulate the channel-wise activations, highlighting important channels and suppressing unrelated ones. The channel attention

mechanism allows the network to adaptively assign weights to dissimilar channels founded on their relevance, promoting the learning of discriminative features and improving the network's capability to capture important information.

Channel Attention focuses on modeling interdependencies between channels in a feature map to emphasize informative channels while suppressing less relevant ones. Mathematically, it can be signified as,

$$F_{ca} = \sigma \left(W_{ca} \left(\frac{1}{H * W} \sum_{i=1}^H \sum_{j=1}^W F_{ij} \right) \right) \otimes F. \quad (5)$$

F signifies the input feature map with dimensions H and W . F_{ij} denotes the activations at spatial location (i, j) in the feature map. W_{ca} is a weight matrix for channel attention. σ signifies an activation function such as \square sigmoid. \otimes represents element-wise multiplication. In this equation, the average operation $\frac{1}{H * W} \sum_{i=1}^H \sum_{j=1}^W F_{ij}$

computes the channel-wise statistics, capturing the global context of the feature map. The weight matrix W_{ca} learns the importance of each channel, and the sigmoid activation function σ scales the channel weights between 0 and 1. Finally, the element-wise multiplication (\odot) applies the channel weights to the original feature map F to obtain the channel attention-enhanced feature map F_{ca} . Spatial Attention, however, focuses on highlighting informative spatial regions within an image. It enables the network to selectively attend to relevant image regions while suppressing less important or noisy regions. Given an input feature map, spatial attention mechanisms aim to capture interdependencies across spatial dimensions.

One common approach is to apply a convolutional layer with a small kernel size (e.g., 1x1) to obtain a spatial attention map. The spatial attention map represents a weight for each spatial location, indicating the importance or relevance of that location. The spatial attention map is usually normalized using an activation function (e.g., softmax) to ensure that the weights sum up to 1 and represent the attention distribution across spatial locations. Finally, the attention map is helpful to the original feature map using element-wise multiplication, boosting the activations in relevant spatial regions. Spatial attention allows the system may zero in on specific locations within an image, enabling better localization and capturing fine-grained details that are crucial for tasks like brain image classification. Both channel attention and spatial attention mechanisms can be used individually or combined to enhance the representation power of CNNs, improve feature discrimination, and give the network more fine-grained control over the information it attends to during processing.

Spatial Attention focuses on modeling interdependencies between spatial locations within a feature map to highlight informative regions while suppressing less relevant ones. Mathematically, it can be represented as:

$$F_{sa} = \sigma \left(W_{sa} \left(\frac{1}{C} \sum_{i=1}^H F_c \right) \right) \odot F \quad (6)$$

where: F_c represents the C^{th} channel of the input feature map F with C channels. W_{sa} is a weight matrix for spatial attention.

Similar to channel attention, the spatial attention equation computes the channel-wise statistics $\frac{1}{C} \sum_{i=1}^H F_c$ to capture the spatial context. The weight

matrix W_{sa} learns the importance of each spatial location, and the sigmoid activation function σ scales the spatial weights between 0 and 1. The element-wise multiplication (\odot) applies the spatial weights to the original feature map F to obtain the spatial attention-enhanced feature map F_{sa} . Both channel attention and spatial attention mechanisms can be used individually or combined to enhance the discriminative power of CNNs by emphasizing relevant channels and spatial locations in the feature maps. These attention mechanisms help the network focus on informative features and suppress noise or less relevant information, ultimately improving the network's performance in various computer vision tasks.

In the fully linked layer, we also use 'dropout' technology, which, without introducing a huge number of variables, may efficiently reduce over-fitting. As a loss function, we also use the category cross-entropy.

$$L = - \sum_m t_m \log z_m, \quad (7)$$

where t_m denotes the right label and z_m the system's output, the Adam approach changes network settings and minimizes the loss in real-time. Hyperparameter values for the Patch Convolutional Neural Network (PCNN) and the Dual Attention Aware Octave Convolution (DACN) network for AD detection can vary depending on the specific implementation and dataset. However, here is Table 1, which shows the hyperparameter values for the proposed model and dataset.

Table 1

Hyperparameter Optimization for the Alzheimer's Disease Detection model

Hyperparameter	PCNN	DACN
Learning Rate	0.001	0.001
Number of Convolutional Layers	4	6
Number of Octave Convolution Layers	-	2
Patch Size	64x64	-
Number of Filters	32	64
Dropout Rate	0.5	0.5
Batch Size	64	128
Number of Epochs	50	100
Activation Function	ReLU	ReLU
Optimizer	Adam	Adam

4. Result and Discussion

Several standard metrics were employed to determine their performance in assessing AD Detection and classification models. Accuracy evaluates how well the model consistently makes accurate predictions. Correctly identified cases (true positives and true negatives) are combined and then divided by the total number of occurrences in the dataset to determine the accuracy rate. However, if the dataset has an uneven distribution of classes, the accuracy metric may not be an adequate measure of the model's efficacy.

Practitioners and scholars can learn the accuracy, precision, recall, and overall efficacy of AD Detection and classification models by evaluating their efficacy using these standard metrics for assessment. The performance analysis report of the projected model is exposed in Table 2.

Table 2

Recital analysis of the proposed model

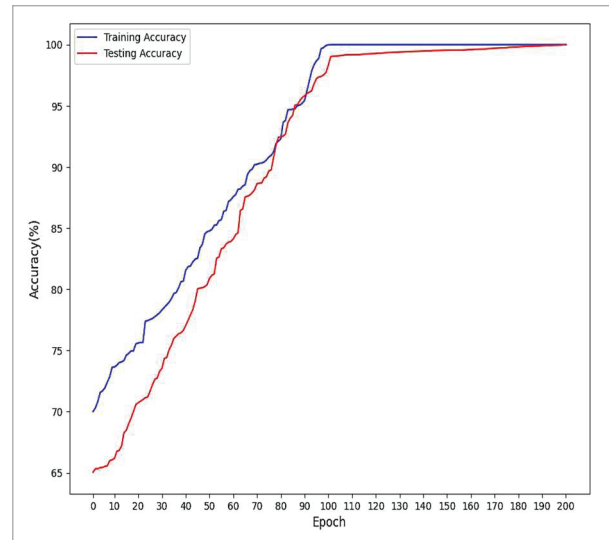
Class	Precision	Recall	F1-score
0	0.99	0.98	0.99
1	1.00	1.00	0.99
2	0.99	0.99	1.00
3	0.98	0.99	0.98
4	0.99	0.98	0.99
Accuracy	99.8		
Micro avg	0.99	0.99	0.99
Weighted avg	0.99	1.00	0.99

In Figure 5, the accuracy of the model for AD Detection is presented. The graph illustrates the training and testing accuracy achieved by the model during the training procedure. According to the graph, the model attained a training accuracy of 100%, indicating that it successfully predicted the correct class for all instances in the training dataset. This high training accuracy proposes that the model has effectively cultured the patterns and features present in the training data.

The testing accuracy, however, is shown to be 99.8%. Indicative of the algorithm's success in making accurate class predictions for instances in the testing dataset that it had not seen during training. Testing accuracy of 99.8% suggests that the model generaliz-

Figure 5

Accuracy of the DACN model for Alzheimer's Disease Detection



es well to unseen data and can effectively classify instances of Alzheimer's disease. The high training and testing accuracy indicate that the model has successfully learned the relevant patterns and features associated with Alzheimer's disease and can accurately classify new instances.

In Figure 6, the loss of the model during the training and testing phases is visualized. The training loss is represented as 0.02, indicating the average loss value

Figure 6

Loss of the DACN model for Alzheimer's Disease Detection

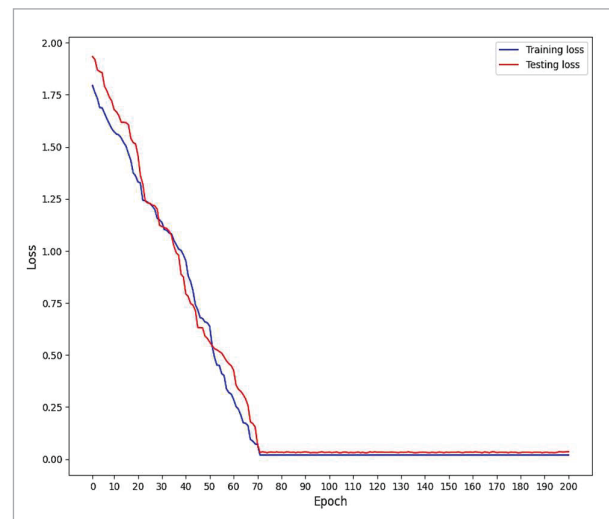
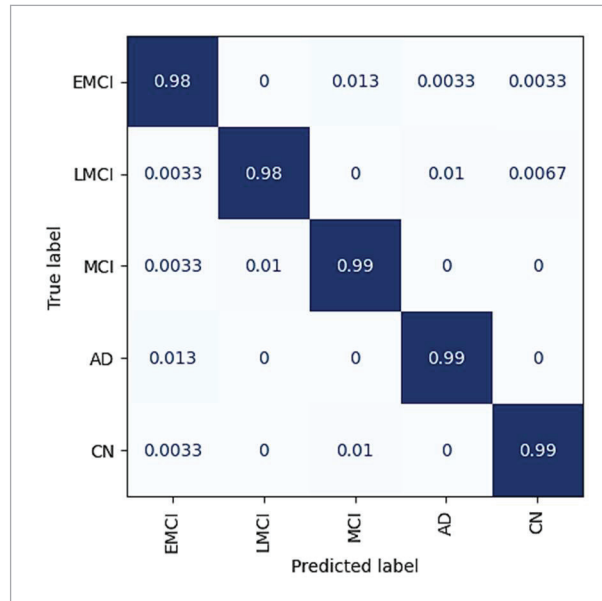


Figure 7

Confusion Matrix of the DACN Model for Alzheimer's Disease Detection



computed during the training process. On the other hand, the testing loss is shown as 0.03, meaning the average loss value is calculated during the testing or evaluation phase. The loss value indicates the model's performance level. It measures how far the model's forecasts deviate from the real ground-truth labels. The closer the model's forecasts are to the actual labels, the smaller the loss value. When the training loss is just 0.02, it is clear that the model is well-fit for the training data since it can reduce the error between anticipated and actual values. Similarly, a testing loss of 0.03 indicates that the model performs well on unobserved data during the testing phase, demonstrating its generalization capability.

Figure 7 presents a confusion matrix to evaluate the model's performance on different classes or categories, namely 'EMCI,' 'LMCI,' 'MCI,' 'AD,' and 'CN.' The confusion matrix is a graphical summary of how well the forecasts made by the model match the actual identifiers. The values in the confusion matrix are expressed as percentages and indicate the accuracy of the model's estimates for each class.

The model achieves an accuracy of 98% for predicting instances belonging to the 'EMCI' class. This means that out of all the cases that are true 'EMCI,' the model correctly classifies 98% of them, while 2% of 'EMCI'

instances are misclassified. The model achieves an accuracy of 98% for predicting instances belonging to the 'LMCI' class. This indicates that out of all the truly 'LMCI,' the model correctly classifies 98% of them, while 2% of 'LMCI' instances are misclassified. The model achieves an accuracy of 99% for predicting instances belonging to the 'MCI' class. This means that out of all the instances that are truly 'MCI,' the model correctly classifies 99% of them, while 1% of 'MCI' instances are misclassified.

The Area Under the ROC Curve (AUC) is a metric that enumerates the overall presentation of the model across all likely thresholds. AUC values range from 0 to 1, where 1 represents a flawless classifier. In our case, the classification model has exceptional performance with a ROC-AUC curve ranging from 0.99 to 1.00, as shown in Figure 8. This indicates that the model achieves near-perfect or perfect discrimination between the positive and negative classes, resulting in high predictive accuracy. AUC values in the range of 0.99 to 1.00 suggest that the model has excellent predictive power and can effectively differentiate between different classes.

Figure 8

The DACN model's ROC and Area Under the Curve for Classifying Alzheimer's

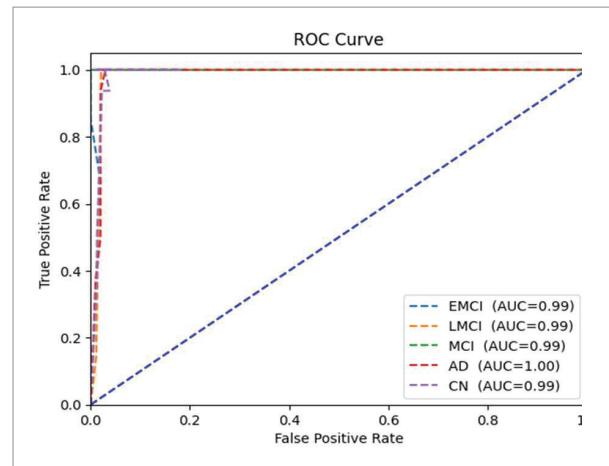


Table 3 summarizes the findings of an analysis of the suggested model and the baseline models used to analyze the same dataset. The table presents the performance metrics of different models, including CNN, LSTM, Bi-LSTM, CLSTM, ResNet50, and the proposed model. The metrics evaluated are accu-

Table 3

Performance comparison of the models on the dataset ADNI

Model	Accuracy	Precision	Recall	F1-score
CNN	95.6	0.95	0.94	0.95
LSTM	96.4	0.95	0.96	0.95
Bi-LSTM	94.8	0.95	0.94	0.95
CLSTM	96.9	0.97	0.96	0.97
ResNet50	97.5	0.97	0.96	0.96
Propose model	99.8	0.99	0.99	1.00

racy, precision, recall, and F1-score, which provide insights into the models' classification capabilities. The CNN model achieved an accuracy of 95.6% with precision, recall, and F1-score values of 0.95, 0.94, and 0.95, respectively. The LSTM model performed slightly better, with an accuracy of 96.4% and precision, recall, and F1-score values of 0.95, 0.96, and 0.95, respectively. The Bi-LSTM model achieved an accuracy of 94.8% with similar precision, recall, and F1-score values of 0.95, 0.94, and 0.95.

The CLSTM model showed improved performance, with an accuracy of 96.9% and precision, recall, and F1-score values of 0.97, 0.96, and 0.97. The ResNet50 model demonstrated even higher accuracy, reaching 97.5%, with precision, recall, and F1-score values of 0.97, 0.96, and 0.96. However, the proposed model outperformed all the baseline models, achieving an exceptional accuracy of 99.8%. The precision, recall and F1-score values were also remarkably high at 0.99, 0.99, and 1.00, respectively. This indicates that the proposed model excelled in accurately classifying instances of Alzheimer's

mer's disease, exhibiting superior performance compared to the baseline models. The results highlight the superiority of the proposed model in terms of accuracy and classification metrics. It demonstrates the model's ability to effectively identify Alzheimer's disease cases, outperforming other established models such as CNN, LSTM, Bi-LSTM, CLSTM, and ResNet50. These findings suggest that the proposed model holds promise as a highly accurate and reliable tool for AD detection on the given dataset.

Table 4 states various ablation studies in detail. The first model, without patching CNN segmentation on brain images, was done, and Dual Attention Aware Octave Convolution was performed for the final classification. In this model, image patching has not been done. CNN-based segmentation with Dual Attention Aware Octave Convolution has been done. The accuracy of the model is 97.5%, which is lower than the proposed model. Likewise, the second model, octave convolution and dual attention-based CNN, are processed without segmentation. Only images are trained and classified here using octave and double attention CNN. This model obtains 95% of accuracy. The third model is tested without octave convolution; in this model, we obtain an accuracy of 96.7%, which is lower than the first model. We tested dual attention CNN for training the images for the fourth model. In this model, initial neurons extract image features, and then, by further pooling, attention is used for classifying the image. Due to ineffective feature extraction, this model performs very low than other models. However, our proposal achieves better than all other models in the table. It is concluded that patching is the first essential component, followed by octave convolution, which extracts features on low and high

Table 4

Performance of Ablation models

Model	Accuracy	Precision	Recall	F1-score
CNN segmentation (No patching) + Dual Attention Aware Octave Convolution	97.5	96	96	97.4
Octave Convolution+dual attention CNN	97.8	97.3	97.6	97.2
PCNN+DACN	96.7	96.2	95.1	96
DACN	92.4	93.4	93.2	93.6
PCNN+OCTAVE+DACN (PROPOSED)	99.8	0.99	0.99	1.00

frequencies. Patching makes the images more evident by pointing out exact noises in image features. Octave convolution further improves image classification by efficiently capturing high-frequency and low-frequency information in an image. The removal of Octave convolution resulted in a noticeable decrease in the model's efficiency, highlighting its role in optimising computational resources. Conversely, the PCNN contributes to overall performance.

5. Conclusion and Future Work

This study concludes by presenting a deep learning-based method for automatically identifying AD using 3D brain MRI data. The study addresses the significant impact of brain illnesses, particularly AD, on fundamental human capabilities such as thought, speech, and movement. The proposed method, the dual

attention aware Octave convolution-based deep learning network (DACN), offers several key contributions. Firstly, it employs a PCNN to extract discriminative features from MRI patches while enhancing the detection of abnormally altered micro-structures in the brain. Secondly, an Octave convolution reduces spatial redundancy and improves the model's perception of the brain's structural details. Lastly, a dual attention-aware convolution classifier is employed to further analyze the resulting image representation. Experimental results using the publicly available ADNI dataset demonstrate the efficiency of the suggested model. The proposed method achieves an outstanding test accuracy of 99.87% for categorizing dementia phases, surpassing the recital of state-of-the-art models. This remarkable accuracy underscores the potential of the DACN model in accurately identifying Alzheimer's disease at an early stage. In future different datasets for AD can be implemented and tested for improving accuracy by cross verification.

References

- Ahmed, S., Choi, K. Y., Lee, J. J., Kim, B. C., Kwon, G. R., Lee, K. H., Jung, H. Y. Ensembles of Patch-Based Classifiers for Diagnosing Alzheimer's Diseases. *IEEE Access*, 2019, 7, 73373-73383. <https://doi.org/10.1109/ACCESS.2019.2920011>
- Balaji, P., Chaurasia, M. A., Bilfaqih, S. M., Muniasamy, A., Alsid, L. E. G. Hybridized Deep Learning Approach for Detecting Alzheimer's Disease. *Biomedicines*, 2023, 11(1), 149. <https://doi.org/10.3390/biomedicines11010149>
- Ben Ahmed, O., Benois-Pineau, J., Allard, M., Ben Amar, C., Catheline, G. Alzheimer's Disease Neuroimaging Initiative. Classification of Alzheimer's Disease Subjects from MRI Using Hippocampal Visual Features. *Multimedia Tools and Applications*, 2015, 74, 1249-1266. <https://doi.org/10.1007/s11042-014-2123-y>
- Braak, H., Braak, E. Frequency of Stages of Alzheimer-related Lesions in Different Age Categories. *Neurobiology of Aging*, 1997, 18(4), 351-357. [https://doi.org/10.1016/S0197-4580\(97\)00056-0](https://doi.org/10.1016/S0197-4580(97)00056-0)
- Chen, Y., Fang, H., Xu, B., Yan, Z., Kalantidis, Y., Rohrbach, M., Yan, S., Feng, J. Drop an Octave: Reducing Spatial Redundancy in Convolutional Neural Networks with Octave Convolution. *arXiv 2019, arXiv:1904.05049*. <https://doi.org/10.1109/ICCV.2019.00353>
- Dominy, S. S., Lynch, C., Ermini, F., Benedyk, M., Marczyk, A., Konradi, A., Nguyen, M., Haditsch, U., Raha, D., Griffin, C. Porphyromonas Gingivalis in Alzheimer's Disease Brains: Evidence for Disease Causation and Treatment with Small-Molecule Inhibitors. *Sci. Adv.* 2019, 5(1), eaau3333. <https://doi.org/10.1126/sciadv.aau3333>
- El-Dahshan, E. S. A., Hosny, T., Salem, A. B. M. Hybrid Intelligent Techniques for MRI Brain Images Classification. *Digital Signal Processing*, 2010, 20(2), 433-441. <https://doi.org/10.1016/j.dsp.2009.07.002>
- Fisher, D. W., Bennett, D. A., Dong, H. Sexual Dimorphism in Predisposition to Alzheimer's Disease. *Neurobiology of Aging*, 2018, 70, 308-324. <https://doi.org/10.1016/j.neurobiolaging.2018.04.004>
- Förstl, H., Levy, R. On Certain Peculiar Diseases of Old Age. *History of Psychiatry*, 1991, 2, 71-101. <https://doi.org/10.1177/0957154X9100200505>
- Gaugler, J., James, B., Johnson, T., Marin, A., Weuve, J. Alzheimer's Disease Facts and Figures. *Alzheimer's Dementia*, 2019, 15(3), 321-387. <https://doi.org/10.1016/j.jalz.2019.01.010>
- Gray, K. R., Aljabar, P., Heckemann, R. A., Hammers, A. NeuroImage Random Forest-based Similarity Measures for Multi-Modal Classification of Alzheimer's Disease. *Neuroimage*, 2013, 65, 167-175. <https://doi.org/10.1016/j.neuroimage.2012.09.065>

12. Helaly, H. A., Badawy, M., Haikal, A. Y. Deep Learning Approach for Early Detection of Alzheimer's Disease. *Cognitive Computing*, 2021, 21,1-17. <https://doi.org/10.1007/s12559-021-09946-2>
13. Hinrichs, C., Singh, V., Mukherjee, L., Xu, G., Chung, M. K., Johnson, S. C. Spatially Augmented LPboosting for AD Classification with Evaluations on the ADNI Dataset. *Neuroimage*, 2009, 48, 138-149. <https://doi.org/10.1016/j.neuroimage.2009.05.056>
14. Hosny, A., Parmar, C., Quackenbush, J., Schwartz, L. H., Aerts, H. J. W. L. Artificial Intelligence in Radiology. *Nature Reviews Cancer*, 2018, 18, 500-510. <https://doi.org/10.1038/s41568-018-0016-5>
15. Hosseini-Asl, E., Keynton, R., El-Baz, A. Alzheimer's Disease Diagnostics by Adaptation of 3D Convolutional Network. In *Proceedings of the International Conference on Image Processing*, Arizona, AZ, USA, 25-28 September 2016, 126-130. <https://doi.org/10.1109/ICIP.2016.7532332>
16. Huang, C., Slovin, P. N., Nielsen, R. B., Skimming, J. W. Diprivan Attenuates the Cytotoxicity of Nitric Oxide in Cultured Human Bronchial Epithelial Cells. *Intensive Care Medicine*, 2002, 28, 1145-1150. <https://doi.org/10.1007/s00134-002-1380-9>
17. Itzhaki, R. Herpes Simplex Virus Type 1, Apolipoprotein E and Alzheimer' Disease. *Herpes: The Journal of the IHMF*, 2004, 11, 77A-82A.
18. Jagadeesh Kumar, S. J. K., Parthasarathi, P., Mofreh A. Hogo., Mehedi Masud., Jehad F. Al-Amri., Mohamed Abouhawwash. Breast Cancer Detection Using Breastnet-18 Augmentation with Fine Tuned Vgg-16. *Intelligent Automation and Soft Computing*, 2023, 36(2), 2363-2378. <https://doi.org/10.32604/iasc.2023.033800>
19. Khagi, B., Kwon, G.R., Lama, R. Comparative Analysis of Alzheimer's Disease Classification by CDR Level Using CNN, Feature Selection, and Machine-Learning Techniques. *The International Journal of Imaging Systems and Technology*, 2019, 29, 1-14. <https://doi.org/10.1002/ima.22316>
20. Khalaf, O. I., Abdulsahib, G. M., Sabbar, B. M. Optimization of Wireless Sensor Network Coverage Using the Bee Algorithm. *Journal of Information Science and Engineering*, 2020, 36, 377-86.
21. Klöppel, S., Stonnington, C. M., Chu, C., Draganski, B., Scahill, R. I., Rohrer, J. D., Fox, N. C., Jack, C. R., Ashburner, J., Frackowiak, R. S. J. Automatic Classification of MR Scans in Alzheimer's Disease. *Brain*, 2008, 131, 681-689. <https://doi.org/10.1093/brain/awm319>
22. Litjens, G., Kooi, T., Bejnordi, B. E., Arindra, A., Setio, A., Ciompi, F., Ghafoorian, M., Van Der Laak, J. A. W. M., Van Ginneken, B., Clara, I. S. A Survey on Deep Learning in Medical Image Analysis. *Medical Image Analysis*, 2017, 42, 60-88. <https://doi.org/10.1016/j.media.2017.07.005>
23. Marcus, D. S., Wang, T. H., Parker, J., Csernansky, J. G., Morris, J. C., Buckner, R. L. Open Access Series of Imaging Studies (oasis): Crosssectional MRI Data in Young, Middle Aged, Nondemented, and Demented Older Adults. *Journal of Cognitive Neuroscience*, 2007, 19(9), 1498-1507. <https://doi.org/10.1162/jocn.2007.19.9.1498>
24. Martinez Murcia, F. J., Ortiz, A., Gorriz, J. M., Ramirez, J., Castillo, Barnes, D. Studying the Manifold Structure of Alzheimer's Disease: A Deep Learning Approach using Convolutional Autoencoders. *IEEE Journal of Biomedical and Health Informatics*, 2020, 24, 17-26. <https://doi.org/10.1109/JBHI.2019.2914970>
25. Morra, J. H., Tu, Z., Apostolova, L. G., Green, A. E., Toga, A. W., Thompson, P. M. Comparison of Adaboost and Support Vector Machines for Detecting Alzheimer's Disease through Automated Hippocampal Segmentation. *IEEE Transactions on Medical Imaging*, 2010, 29, 30-43. <https://doi.org/10.1109/TMI.2009.2021941>
26. Neffati, S., Ben Abdellafou, K., Jaffel, I., Taouali, O., Bouzrara, K. An Improved Machine Learning Technique based on Downsized KPCA for Alzheimer's Disease Classification. *The International Journal of Imaging Systems and Technology*, 2019, 29, 121-131. <https://doi.org/10.1002/ima.22304>
27. Niu, H., Álvarez-Álvarez, I., Guillén-Grima, F., Aguinaga-Ontoso, I. Prevalence and Incidence of Alzheimer's Disease in Europe: A Meta-Analysis. *Neurología*, 2017, 32(8), 523-532. <https://doi.org/10.1016/j.nrleng.2016.02.009>
28. Odusami, M., Maskeliūnas, R., Damaševičius, R. An Intelligent System for Early Recognition of Alzheimer's Disease using Neuroimaging. *Sensors*, 2022, 22(3). <https://doi.org/10.3390/s22030740>
29. Odusami, M., Maskeliūnas, R., Damaševičius, R. Pixel-Level Fusion Approach with Vision Transformer for Early Detection of Alzheimer's Disease. *Electronics (Switzerland)*, 2023, 12(5). <https://doi.org/10.3390/electronics12051218>
30. Prajapati, R., Khatri, U., Kwon, G. R. An Efficient Deep Neural Network Binary Classifier for Alzheimer's Disease Classification. In: *International Conference on Artificial Intelligence in Information and Communication (ICAIIIC)*, 2021, 231-234. <https://doi.org/10.1109/ICAIIIC51459.2021.9415212>
31. Rallabandi, V. S., Tulpule, K., Gattu, M. Alzheimer's Disease Neuroimaging Initiative. Automatic Classification of Cognitively Normal, Mild Cognitive Impairment and

- Alzheimer's Disease using Structural MRI Analysis. *Informatics in Medicine Unlocked*, 2020, 18, 100305. <https://doi.org/10.1016/j.imu.2020.100305>
32. Razzak, I., Naz, S., Alinejad-Rokny, H., Nguyen, T. N., Khalifa, F. A Cascaded Multiresolution Ensemble Deep Learning Framework for Large Scale Alzheimer's Disease Detection Using Brain MRIs. *IEEE/ACM Transactions on Computational Biology and Bioinformatics*, 2022. <https://doi.org/10.1109/TCBB.2022.3219032>
33. Ritchie, K., Ritchie, C. W. Mild Cognitive Impairment (MCI) Twenty Years on. *International Psychogeriatrics*, 2012, 24, 1-5. <https://doi.org/10.1017/S1041610211002067>
34. Sarraf, S., DeSouza, D. D., Anderson, J., Tofghi, G. Alzheimer's Disease Neuroimaging Initiative. DeepAD: Alzheimer's disease classification via deep convolutional neural networks using MRI and fMRI. *BioRxiv*, 2016, 070441. <https://doi.org/10.1101/070441>
35. Strassnig, M., Ganguli, M. About a Peculiar Disease of the Cerebral Cortex: Alzheimer's Original Case Revisited. *Psychiatry (Edgmont)*, 2005, 2(9), 30.
36. Uysal, G., Ozturk, M. Classifying Early and Late Mild Cognitive Impairment Stages of Alzheimer's Disease by Analyzing Different Brain Areas. In *Proceedings of the 2020 Medical Technologies Congress (TIPTEKNO)*, Antalya, Turkey, 19-20 November 2020, 1-4. <https://doi.org/10.1109/TIPTEKNO50054.2020.9299217>
37. Wurts, A., Oakley, D. H., Hyman, B. T., Samsi, S. Segmentation of Tau Stained Alzheimers Brain Tissue Using Convolutional Neural Networks. In *Proceedings of the 2020 42nd Annual International Conference of the IEEE Engineering in Medicine & Biology Society (EMBC)*, Montreal, QC, Canada, 20-24 July 2020, 1420-1423. <https://doi.org/10.1109/EMBC44109.2020.9175832>
38. Xie, Q., Zhao, W., Ou, G., Xue, W. An Overview of Experimental and Clinical Spinal Cord Findings in Alzheimer's Disease. *Brain Sciences*, 2019, 9, 168. <https://doi.org/10.3390/brainsci9070168>
39. Yue, L., Gong, X., Li, J., Ji, H., Li, M., Nandi, A. K. Hierarchical Feature Extraction for Early Alzheimer's Disease Diagnosis. *IEEE Access*, 2019, 7, 93752-93760. <https://doi.org/10.1109/ACCESS.2019.2926288>
40. Zhang, Y., Wang, S. Detection of Alzheimer's Disease by Displacement Field and Machine Learning. *PeerJ*, 2015, 3, 1-29. <https://doi.org/10.7717/peerj.1251>

